

Spectroscopic parameters and electromagnetic form factor of kaon in vacuum and a dense medium

N. Er^{1,*} and K. Azizi^{2,3,†}

¹*Department of Physics, Bolu Abant İzzet Baysal University, Gököy Kampüsü, 14030 Bolu, Turkey*

²*Department of Physics, University of Tehran, North Karegar Ave. Tehran 14395-547, Iran*

³*Department of Physics, Doğuş University, Dudullu-Ümraniye, 34775 Istanbul, Turkey*

(Dated: April 28, 2022)

The spectroscopic parameters as well as electromagnetic form factor of the strange particle kaon are investigated in vacuum and a medium with finite density. The obtained vacuum mass and decay constant, which are consistent with the existing experimental results, are used to extract the Q^2 dependence of the kaon electromagnetic form factor in the interval $Q^2 \in [0, 10]$ GeV² in vacuum. The obtained results at lower and intermediate values of Q^2 are consistent with the existing experimental data within the presented uncertainties. The Q^2 behavior of the electromagnetic form factor of kaon in vacuum and in the interval $Q^2 \in [0, 6]$ GeV² is in a nice agreement with the existing predictions of the Lattice QCD and the solution of the Bethe-Salpeter equation for the model of Nambu and Jona-Lasinio (NJL) with proper-time regularization, as well. The obtained vacuum radius for kaon is also in a nice agreement with the world's average experimental result. We extend the analyses to a medium with higher densities and obtain the behavior of the mass, decay constant, electromagnetic form factor and radius with respect to density. The obtained results for some of the parameters are compared with the existing predictions of other models and approaches. The results obtained in the present study can be useful for future experimental and theoretical studies both in vacuum and a dense medium.

I. INTRODUCTION

Investigation of the light pseudoscalar mesons with spin-parity $J^P = 0^-$ plays an important role for a better understanding of the perturbative and nonperturbative natures of Quantum Chromodynamics (QCD). The spectroscopic properties of these particles have been widely studied theoretically and experimentally in vacuum. Although, there have been many efforts to study the electromagnetic form factors, inner charge and magnetization distributions and mechanical properties of these particles such as their radius, we still need more experimental and theoretical studies to clarify the obtained results in vacuum. Theoretical calculations of the above mentioned parameters in a dense medium can be very useful for analyses of the future data provided by the in-medium experiments.

In terms of experimental studies, the simplest particles among light mesons are the pion triplet. In the last years, the static properties and dynamical features of pions have been extensively studied in many works [1–14]. The next simple meson available for experimental studies is the strange particle, kaon, but there are relatively fewer studies devoted to the study of parameters of kaons [15–24].

The electromagnetic properties such as electromagnetic form factors (FFs) of particles carry useful information about the distributions of the charge and magnetization, determination of which can help us obtain valu-

able knowledge on the internal structure of hadrons in terms of quark-gluon organizations and their geometric shapes. Theoretical calculations as well as experimental studies on the electromagnetic properties of nucleons and light mesons are done by different collaborations and experimental groups. Different groups consider different ranges for the transferred momentum squared Q^2 carried by the electromagnetic current. We need to extract the FFs in a wide range of Q^2 to get a complete knowledge on the FFs of hadrons. In the present study, we determine the FFs of the strange meson K^+ in the interval $Q^2 \in [0, 10]$ GeV² using the QCD sum rules in vacuum. The mass and decay constant of the kaon are entered as the main input parameters to the calculations. We use vacuum two-point sum rules to extract these spectroscopic parameters. We discuss the behavior of the kaon electromagnetic form factor with respect to Q^2 and compare the obtained results with the existing experimental data and predictions of other theoretical and phenomenological models. We calculate the vacuum charge radius of K^+ particle and compare the result with the experimental data and existing theoretical predictions.

Investigation of hadronic parameters at a dense medium, on the other hand, is very important to complete our knowledge on the nature and structure of hadrons both theoretically and experimentally. By the progresses made in the experimental side, we hope it will be possible to study the statistic and dynamical properties of hadrons in future in-medium experiments. Motivated by this, in the present study, we extend our calculations on the spectroscopic parameters as well as electromagnetic FFs and charge radius of K^+ to a dense medium and discuss the variations of these hadronic parameters with respect to the density of the medium. To

*Electronic address: nuray@ibu.edu.tr

†Electronic address: kazem.azizi@ut.ac.ir (Corresponding Author)

obtain our results we use the two-point in-medium sum rules for the spectroscopic parameters and three-point in-medium sum rules for the in-medium electromagnetic interaction to extract the electromagnetic FFs. There are some limited information on some of these parameters available in the literature that we compare our results with these information.

The paper is organized in the following way. In next section, we calculate the mass and decay constant of K^+ both in vacuum and a dense medium and obtain their numerical values. In section III, we calculate the electromagnetic form factor and charge radius of K^+ again in vacuum and a dense medium and perform our numerical analyses. Last section is devoted to the summary and our concluding notes.

II. THE SPECTROSCOPIC PARAMETERS OF KAON IN VACUUM AND A DENSE MEDIUM

The in-medium time-ordered two point correlation amplitude $\Pi_{\mu\nu}$, responsible for the calculation of mass and decay constant of kaon, is given as

$$\Pi_{\mu\nu} = i \int d^4x e^{ip \cdot x} \langle \psi_0 | \mathcal{T} [j_\mu(x) j_\nu^\dagger(0)] | \psi_0 \rangle, \quad (1)$$

where $|\psi_0\rangle$ is the ground state of the nuclear medium. For the vacuum calculations, this state is replaced with the vacuum one $|0\rangle$. The interpolating current of kaon in Eq. (1) is

$$j_\mu(x) = \bar{s}^a(x) \gamma_\mu \gamma_5 u^a(x), \quad (2)$$

and \mathcal{T} denotes the time ordered product of two currents.

In accordance with the QCD sum rule method, the correlation function in Eq. (1) can be represented in terms of hadronic parameters called the physical or hadronic side, and alternatively in terms of the QCD degrees of freedom called the QCD side. The hadronic side is obtained in terms of the in-medium decay constant f_K^* and mass m_K^* of kaon. The axial current considered for the kaon simultaneously couples to both the pseudoscalar (PS) and axial vector (AV) kaons. Hence, after performing the four space-time integral and isolating these two states, we get

$$\begin{aligned} \Pi_{\mu\nu}^{Phys} &= \frac{\langle \psi_0 | j_\mu | K_{AV}(p^*) \rangle \langle K_{AV}(p^*) | j_\nu^\dagger | \psi_0 \rangle}{m_{AV}^{*2} - p^{*2}} \\ &+ \frac{\langle \psi_0 | j_\mu | K_{PS}(p^*) \rangle \langle K_{PS}(p^*) | j_\nu^\dagger | \psi_0 \rangle}{m_{PS}^{*2} - p^{*2}} + \dots, \end{aligned} \quad (3)$$

where dots stand for contributions of the higher resonances and continuum states in both the PS and AV channels. The in-medium momentum is given as $p_\mu^* = p_\mu - \Sigma_\nu u_\mu$, where Σ_ν is the vector self-energy and u_μ is the four-velocity of the nuclear medium. We shall work in the rest frame of the medium, $u_\mu = (1, 0)$.

To simplify the above relation, we define the corresponding matrix elements in terms of the in-medium masses, decay constants, momenta and polarization vector of AV state:

$$\begin{aligned} \langle \psi_0 | j_\mu | K_{AV}(p^*) \rangle &= f_{AV}^* m_{AV}^* \epsilon_\mu^*, \\ \langle \psi_0 | j_\mu | K_{PS}(p^*) \rangle &= f_{PS}^* m_{PS}^* p_\mu^*. \end{aligned} \quad (4)$$

In vacuum, the in-medium masses, decay constants and momenta as well as the polarization vector of axial kaon are replaced by their vacuum versions without stars. Using Eq. (4) in Eq. (3) leads to

$$\begin{aligned} \Pi_{\mu\nu}^{Phys} &= \frac{f_{AV}^{*2} m_{AV}^{*2}}{m_{AV}^{*2} - p^{*2}} \left[-g_{\mu\nu} + \frac{p_\mu^* p_\nu^*}{p^{*2}} \right] \\ &+ \frac{f_{PS}^{*2} m_{PS}^{*2} p_\mu^* p_\nu^*}{m_{PS}^{*2} - p^{*2}} + \dots \end{aligned} \quad (5)$$

We need to extract the contribution of PS state only. To remove axial particle contributions in Eq. (5) we multiply the physical side by $\frac{p_\mu p_\nu}{p^2}$ for vacuum and p_μ^* for in-medium cases. In the dense medium, we need more structures and some rules to find some parameters beyond the vacuum: like the vector self energy. Constructing more sum rules allows us to simultaneously find the mass, decay constant and vector self energy of the particle. The Borel transformation with respect to momentum squared is applied to suppress the contributions of the higher states and continuum. After removing the contributions of AV states and performing the standard calculations, the Borel transformed physical side for vacuum and dense medium are obtained as

$$\hat{\mathbf{B}} \left[\frac{p_\mu p_\nu}{p^2} \Pi_{\mu\nu}^{Phys} \right] = f_{PS}^2 m_{PS}^4 e^{-m_{PS}^2/M^2} \mathbf{I}, \quad (6)$$

and

$$\hat{\mathbf{B}} [p_\mu^* \Pi_{\mu\nu}^{Phys}] = f_{PS}^{*2} m_{PS}^{*4} e^{-\mu^2/M^2} (p_\nu - \Sigma_\nu u_\nu), \quad (7)$$

where $\mu^2 = m_{PS}^{*2} - \Sigma_\nu^2 + 2\Sigma_\nu p_0$, M^2 is the Borel mass parameter, p_0 is the energy of the quasi-particle in medium and \mathbf{I} denotes the unit matrix.

On the other hand, the correlation function in Eq. (1) can be calculated in terms of quarks and gluon degrees of freedom in deep Euclidean region. Using the current in Eq. (2) and contracting the light quark fields in Eq. (1), we obtain the QCD side of the correlation function as

$$\Pi_{\mu\nu}^{QCD} = i \int d^4x e^{ip \cdot x} Tr[\gamma_5 S_u^{ab}(x) \gamma_5 \gamma_\nu S_s^{ba}(-x) \gamma_\mu], \quad (8)$$

where $S_{q=u(s)}$ is the full color carried light quark propagator in the dense medium. It can be expanded as,

$$\begin{aligned} S_q^{kl}(x) &= \left(\frac{i}{2\pi^2} \frac{\not{x}}{x^4} - \frac{m_q}{4\pi^2 x^2} + i \frac{m_q^2}{8\pi^2} \frac{\not{x}}{x^2} \right) \delta^{kl} + \chi_q^k(x) \bar{\chi}_q^l(0) \\ &- i \frac{g_s}{32\pi^2} \frac{\not{x} \sigma_{\mu\nu} + \sigma_{\mu\nu} \not{x}}{x^2} F_A^{\mu\nu}(0) t_A^{kl} + \dots, \end{aligned} \quad (9)$$

where the term inside the parenthesis is the perturbative part and the second and the third terms represent the non-perturbative contributions. Here, χ_q^k and $\bar{\chi}_q^l$ are the Grassmann background quark fields, $F_A^{\mu\nu}$ is the background gluon field and $t_A^{kl} = \frac{\lambda_A^{kl}}{2}$ with λ_A^{kl} being the Gell-Mann matrices.

To proceed in QCD side we shall put the full expressions of the two propagators in Eq. (8), which leads to a result containing a perturbative part and a nonperturbative part including different in-medium quark, gluon and mixed condensates, which are functions of the density of the nuclear matter (ρ). We do not present all the steps in calculations, but refer the reader to, for instance, Ref. [25] for details. After using all the in-medium operators presented in Ref. [25], we need to transfer the calculations to the momentum space. For this, we use

$$\frac{1}{(x^2)^n} = \int \frac{d^D t}{(2\pi)^D} e^{-it \cdot x} i(-1)^{n+1} 2^{D-2n} \pi^{D/2} \times \frac{\Gamma[D/2 - n]}{\Gamma[n]} \left[-\frac{1}{t^2} \right]^{D/2-n}, \quad (10)$$

in D dimension. We also use, $x_\mu \rightarrow -i \frac{\partial}{\partial p_\mu}$ for those x_μ that appear in nominators of different terms. The next step is to perform the Fourier integral over x , as a result of which a Dirac Delta function including the momentum of the particle p and t , originated from the above relation, appears. Using the resultant Dirac Delta, we perform the D -dimensional integral over t . This leads us to some expressions in momentum space. We set $D = 4 - 2\epsilon$ and perform dimensional regularization. Then, we apply the standard Borel transformation in order to suppress the contributions of the higher states and continuum. Finally, the following replacement is used to apply the continuum subtraction procedure:

$$(M^2)^N e^{-m^2/M^2} \rightarrow \frac{1}{\Gamma(N)} \int_{m^2}^{s_0} ds e^{-s/M^2} (s - m^2)^{N-1}, \quad (11)$$

for $N > 0$, where s_0 is the continuum threshold to be fixed based on the standard prescriptions of the method later. As a result of the above procedures, the following relations for the QCD sides of the vacuum and in-medium cases are obtained:

$$\begin{aligned} \hat{\mathbf{B}}\left[\frac{p_\mu p_\nu}{p^2} \Pi_{\mu\nu}^{QCD}\right] &= \mathbf{\Omega}(M^2, s_0) \mathbf{I}, \\ \hat{\mathbf{B}}\left[p_\mu^* \Pi_{\mu\nu}^{QCD}\right] &= \mathbf{\Omega}_1^*(M^2, s_0, \rho) p_\nu + \mathbf{\Omega}_2^*(M^2, s_0, \rho) u_\nu, \end{aligned} \quad (12)$$

where $\mathbf{\Omega}(M^2, s_0)$, $\mathbf{\Omega}_1^*(M^2, s_0, \rho)$ and $\mathbf{\Omega}_2^*(M^2, s_0, \rho)$ are the Borel transformed amplitudes of the corresponding structures. The expressions of these functions are very lengthy and we do not present their explicit forms for simplicity.

The sum rules for the mass and decay constant of pseudoscalar state in vacuum and these quantities together with the vector self-energy of the particle in medium are

obtained by equating the coefficients of the same structures from both the physical and QCD sides for each case. In vacuum we obtain the sum rule

$$f_K^2 m_K^4 e^{-m_K^2/M^2} = \mathbf{\Omega}(M^2, s_0), \quad (13)$$

which leads to

$$\begin{aligned} m_K^2 &= \frac{\mathbf{\Omega}'(M^2, s_0)}{\mathbf{\Omega}(M^2, s_0)}, \\ f_K^2 &= \frac{\mathbf{\Omega}(M^2, s_0)}{m_K^4} e^{m_K^2/M^2}, \end{aligned} \quad (14)$$

for the mass and decay constant of the K meson in vacuum, where $\mathbf{\Omega}'(M^2, s_0) = \frac{d\mathbf{\Omega}(M^2, s_0)}{d(-1/M^2)}$. We also obtain the following density dependent sum rules for the mass, decay constant and vector self-energy of kaon in medium:

$$\begin{aligned} f_{PS}^{*2} m_{PS}^{*4} e^{-\mu^2/M^2} &= \mathbf{\Omega}_1^*(M^2, s_0, \rho), \\ -f_{PS}^{*2} m_{PS}^{*4} \Sigma_v e^{-\mu^2/M^2} &= \mathbf{\Omega}_2^*(M^2, s_0, \rho), \\ \Sigma_v &= -\frac{\mathbf{\Omega}_2^*(M^2, s_0, \rho)}{\mathbf{\Omega}_1^*(M^2, s_0, \rho)}. \end{aligned} \quad (15)$$

These sum rules are used to obtain the numerical values of the vacuum and in-medium physical quantities of kaon. For this, besides the mass of light quarks taken from Ref. [26], the parameters of vacuum and in-medium quark, gluon and mixed condensates with different dimensions and saturation nuclear matter density are needed (see for instance Ref. [25] and references therein) :

$$\begin{aligned} m_u &= 2.16_{-0.26}^{+0.49} \text{ MeV}, m_s = 93_{-5}^{+11} \text{ MeV}, \\ \rho^{sat} &= (0.11)^3 \text{ GeV}^3, \langle q^\dagger q \rangle_\rho = \frac{3}{2} \rho_N, \langle s^\dagger s \rangle_\rho = 0, \\ \langle \bar{q}q \rangle_0 &= (-0.241)^3 \text{ GeV}^3, \langle \bar{s}s \rangle_0 = 0.8 \langle \bar{q}q \rangle_0, \\ \langle \bar{q}q \rangle_\rho &= \langle \bar{q}q \rangle_0 + \frac{\sigma_N}{2m_q} \rho, \\ \sigma_N &= 0.059 \text{ GeV}, m_q = 0.00345 \text{ GeV}, \\ \langle \bar{s}s \rangle_\rho &= \langle \bar{s}s \rangle_0 + y \frac{\sigma_N}{2m_q} \rho, y = 0.05 \pm 0.01, \\ \langle \frac{\alpha_s}{\pi} G^2 \rangle_0 &= (0.33 \pm 0.04)^4 \text{ GeV}^4, \\ \langle \frac{\alpha_s}{\pi} G^2 \rangle_\rho &= \langle \frac{\alpha_s}{\pi} G^2 \rangle_0 - (0.65 \pm 0.15) \text{ GeV} \rho, \\ \langle q^\dagger i D_0 q \rangle_\rho &= 0.18 \text{ GeV} \rho_N, \\ \langle s^\dagger i D_0 s \rangle_\rho &= \frac{m_s \langle \bar{s}s \rangle_\rho}{4} + 0.02 \text{ GeV} \rho, \\ \langle \bar{q} i D_0 q \rangle_\rho &= \langle \bar{s} i D_0 s \rangle_\rho = 0, \\ \langle \bar{q} g_s \sigma G q \rangle_0 &= m_0^2 \langle \bar{q}q \rangle_0, \langle \bar{s} g_s \sigma G s \rangle_0 = m_0^2 \langle \bar{s}s \rangle_0, \\ m_0^2 &= 0.8 \text{ GeV}^2, \langle \bar{q} g_s \sigma G q \rangle_\rho = \langle \bar{q} g_s \sigma G q \rangle_0 + 3 \text{ GeV}^2 \rho, \\ \langle \bar{s} g_s \sigma G s \rangle_\rho &= \langle \bar{s} g_s \sigma G s \rangle_0 + 3y \text{ GeV}^2 \rho, \\ \langle q^\dagger g_s \sigma G q \rangle_\rho &= -0.33 \text{ GeV}^2 \rho, \\ \langle q^\dagger i D_0 i D_0 q \rangle_\rho &= 0.031 \text{ GeV}^2 \rho_N - \frac{1}{12} \langle q^\dagger g_s \sigma G q \rangle_\rho, \\ \langle s^\dagger g_s \sigma G s \rangle_\rho &= -0.33y \text{ GeV}^2 \rho, \\ \langle s^\dagger i D_0 i D_0 s \rangle_\rho &= 0.031y \text{ GeV}^2 \rho - \frac{1}{12} \langle s^\dagger g_s \sigma G s \rangle_\rho, \end{aligned} \quad (16)$$

Method		m_K	f_K
PS	QCDSR	$496.5^{+9.7}_{-10.8}$ MeV	$158.1^{+3.2}_{-2.6}$ MeV
[21]	Lattice	-	154.4(2.0) MeV
PDG [26]	Exp	493.677 ± 0.016 MeV	155.6(0.4) MeV
[27]	Lattice	$478 \pm 16 \pm 20$ MeV	$152 \pm 6 \pm 10$ MeV
[28]	Lattice	-	156.3(0.6) MeV
[29]	Lattice	-	155.7(0.3) MeV

TABLE I: Mass and decay constant of K^+ meson in vacuum compared with the Experimental data and Lattice QCD results. PS represents the presents study.

where $\langle \mathcal{O} \rangle_0$, for the corresponding operator \mathcal{O} , is used to represent the vacuum condensates, while $\langle \mathcal{O} \rangle_\rho$ stands for the in-medium condensates.

Some necessary conditions like pole dominance and convergence of the operator product expansion have to be fulfilled in order to fix the working regions for the auxiliary parameters M^2 and s_0 . We also require that the dependence of the physical quantities on these auxiliary parameters be relatively weak. As a result, we can fix the Borel and continuum threshold parameters within the limits:

$$M^2 \in [0.4 - 0.6] \text{ GeV}^2 \ \& \ s_0 \in [0.63 - 0.99] \text{ GeV}^2. \quad (17)$$

Considering these intervals, we plot the M^2 dependence of the kaon decay constant in vacuum in Fig. (1). We observe that the decay constant shows a good stability against the variations of the auxiliary parameters within their working windows. Extracted from the analyses we depict the values of the mass and decay constant of the K^+ meson compared with the experimental data and Lattice QCD predictions in Table I. We see good consistencies among the presented values within the uncertainties.

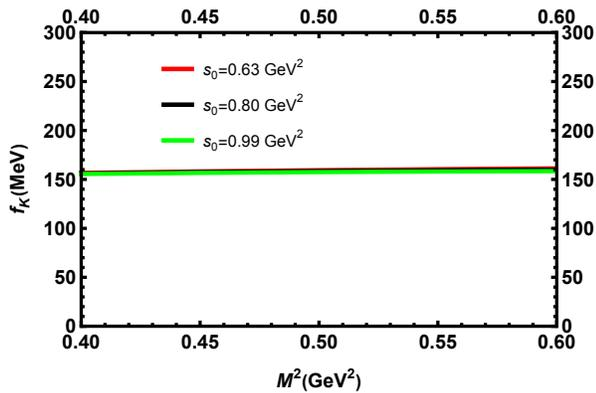


FIG. 1: The decay constant of K^+ meson in vacuum with respect to Borel mass parameter at different continuum thresholds.

We proceed to discuss the dependencies of the considered quantities on the density of the nuclear medium.

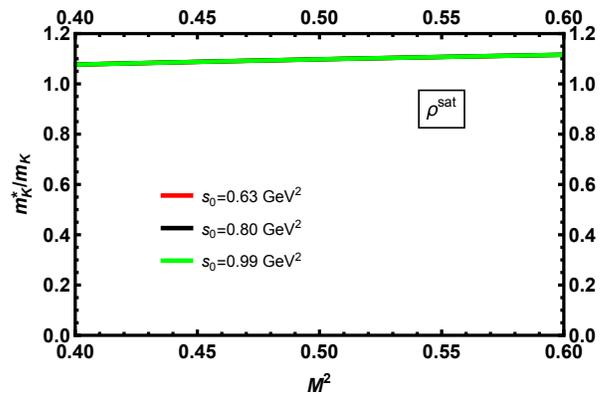


FIG. 2: Variation of the ratio of the in-medium to vacuum mass for K^+ meson with respect to Borel mass parameter at saturation density and different continuum thresholds.

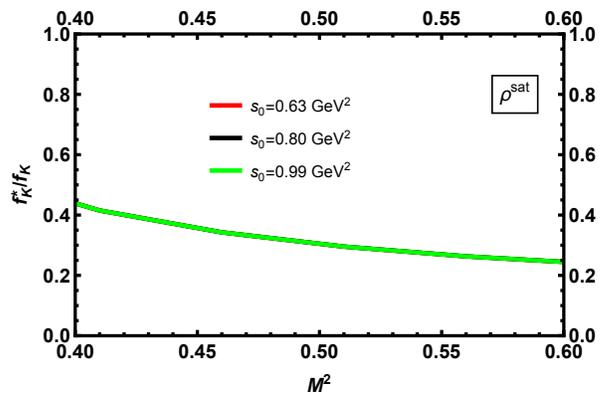


FIG. 3: The same as Fig. 2 but for decay constant of K^+ meson.

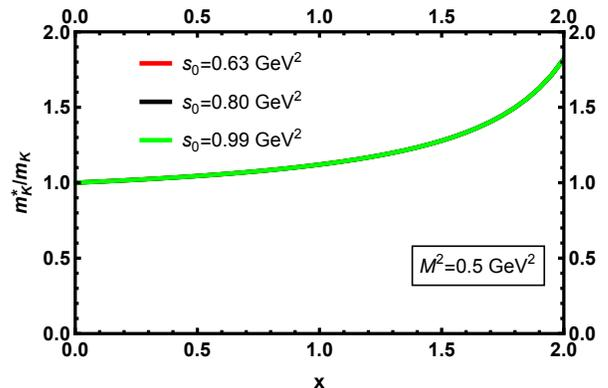


FIG. 4: The density dependence of the ratio of in-medium to vacuum mass for K^+ meson at $M^2 = 0.5 \text{ GeV}^2$ and different continuum thresholds.

To check the stability of the results with respect to the auxiliary parameters, in Figs. (2) and (3), we depict the ratios m_K^*/m_K and f_K^*/f_K as functions of M^2 at different values of s_0 at the saturation nuclear matter density ρ^{sat} . From these figures, we see a good stability of m_K^*/m_K and f_K^*/f_K with respect to the continuum

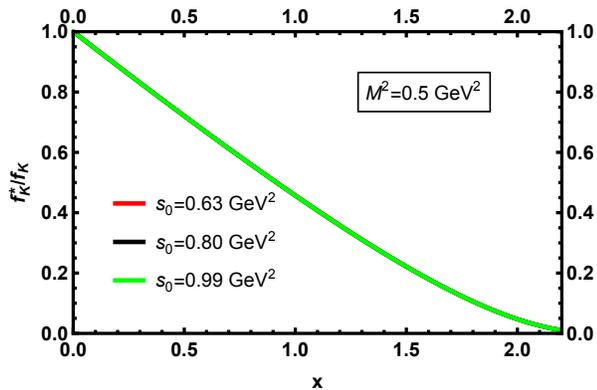


FIG. 5: The same as Fig. 4 but for decay constant of K^+ meson.

Method		m_K^*
PS	QCDSR	553 ± 12 MeV
[30]	Chiral SU(3) model	521 MeV

TABLE II: The in-medium mass of kaon at saturation density.

threshold. The ratio m_K^*/m_K shows a nice stability with respect to M^2 , as well. We see some residual dependence of f_K^*/f_K to M^2 but it remains within the limits allowed by the QCD sum rule method.

The last step in this section is to discuss the dependence of the physical quantities under consideration on the density of the nuclear medium. To this end, in Figs. (4) and (5) we plot the dependence of the ratios m_K^*/m_K and f_K^*/f_K on $x = \rho/\rho^{sat}$. These figure indicate that the mass of K^+ meson increases with the increase in the density, although the rate at lower densities is small. The decay constant linearly decreases with the increase in the density of the medium and it reaches to zero at $\rho \simeq 2.2\rho^{sat}$ and we are witness of the melting of meson at higher densities. At saturation density, the result of the present study for the in-medium mass is compared with the result of Chiral SU(3) model obtained in Ref. [30] (see Table II): Both show considerable growths with respect to the medium mass value. We shall use the density-dependent functions of the mass and decay constant as main inputs in next section to determine the density-dependent electromagnetic form factor and other observables.

III. ELECTROMAGNETIC FORM FACTOR AND CHARGE RADIUS OF KAON IN VACUUM AND A DENSE MEDIUM

The following in-medium three-point correlation function is responsible for extraction of the electromagnetic form factor and charge radius:

$$\Pi_{\mu\nu\lambda} = i^2 \int d^4x \int d^4y e^{ip \cdot x} e^{-ip' \cdot y} \times \langle \psi_0 | \mathcal{T} [j_\mu(y) J_\lambda(0) j_\nu^\dagger(x)] | \psi_0 \rangle, \quad (18)$$

where $p = p' + q$ and p' are the momenta of the initial and final kaonic states, respectively and q is carried by the electromagnetic current. The electromagnetic current is

$$J_\lambda(0) = e_u \bar{u}(0) \gamma_\lambda u(0) + e_d \bar{d}(0) \gamma_\lambda d(0) + e_s \bar{s}(0) \gamma_\lambda s(0), \quad (19)$$

with $e_{u,d,s}$ being the charge of the corresponding quark. Using the axial current and current dagger at two different points for kaon and the electromagnetic current we get the following expression in terms of the quark propagators after applying the Wick's theorem:

$$\begin{aligned} \Pi_{\mu\nu\lambda}^{QCD} &= i^2 \int d^4x \int d^4y e^{ip \cdot x} e^{-ip' \cdot y} \\ &\times \left[e_u \text{Tr} [S_s^{da}(x-y) \gamma_\mu \gamma_5 S_u^{ab}(y) \gamma_\lambda S_u^{bd}(-x) \gamma_5 \gamma_\nu] \right. \\ &\left. + e_s [S_s^{dc}(x) \gamma_\lambda S_s^{ca}(-y) \gamma_\mu \gamma_5 S_u^{ad}(y-x) \gamma_5 \gamma_\nu] \right]_{\psi_0}. \end{aligned} \quad (20)$$

We apply similar procedures as the previous section: The full light quark propagators in medium and vacuum are placed in the above equation and the standard Fourier, double-Borel and continuum subtraction procedures are performed. For simplicity we do not present these lengthy but standard procedures here. As a result of the above procedures, the correlation function in QCD side is obtained.

The physical side of the calculations is obtained by saturation of the correlation function (18) with two complete sets of intermediate states both in the AV and PS channels. Performing the integrals over four- x and four- y , we get

$$\begin{aligned} \Pi_{\mu\nu\lambda}^{Phys} &= \frac{\langle \psi_0 | j_\mu | K^{AV}(p_2^*) \rangle \langle K^{AV}(p_2^*) | J_\lambda | K^{AV}(p_1^*) \rangle \langle K^{AV}(p_1^*) | j_\nu^\dagger | \psi_0 \rangle}{(m_{AV}^{*2} - p_1^{*2})(m_{AV}^{*2} - p_2^{*2})} \\ &+ \frac{\langle \psi_0 | j_\mu | K^{PS}(p_2^*) \rangle \langle K^{PS}(p_2^*) | J_\lambda | K^{PS}(p_1^*) \rangle \langle K^{PS}(p_1^*) | j_\nu^\dagger | \psi_0 \rangle}{(m_{PS}^{*2} - p_1^{*2})(m_{PS}^{*2} - p_2^{*2})} + \dots, \end{aligned} \quad (21)$$

in medium, where $p_1^* = p^*$ and $p_2^* = p'^*$. The vacuum version of this step is obtained by replacing the star quantities

with their without star versions. The transition matrix elements in Eq. (21) are defined in terms of the in-medium form factors as

$$\begin{aligned} \langle K^{AV}(p_2^*) | J_\lambda | K^{AV}(p_1^*) \rangle &= \varepsilon'_\tau(p_2^*) \left[F_1^{*AV}(Q^2) g_{\tau\sigma}(p_{1,\lambda}^* + p_{2,\lambda}^*) + F_2^{*AV}(Q^2) (q_\tau^* g_{\lambda\sigma} - q_\sigma^* g_{\lambda\tau}) \right. \\ &\quad \left. - \frac{F_3^{*AV}(Q^2) q_\tau^* q_\sigma^* (p_{1,\lambda}^* + p_{2,\lambda}^*)}{2m_{AV}^{*2}} \right] \varepsilon_\sigma(p_1^*), \\ \langle K^{PS}(p_2^*) | J_\lambda | K^{PS}(p_1^*) \rangle &= F^{*PS}(Q^2) (p_{1,\lambda}^* + p_{2,\lambda}^*), \end{aligned} \quad (22)$$

where $Q^2 = -q^2$; and ε and ε' are the polarization vectors of the initial and final axial states, respectively. Here, $F_{1,2,3}^{*AV}(Q^2)$ are the axial vector particle and $F^{*PS}(Q^2)$ is the pseudoscalar particle invariant electromagnetic form factors. By using Eq. (22) in Eq. (21), one obtains an expression for $\Pi_{\mu\nu\lambda}^{Phys}$ in terms of the in-medium form factors, polarization vectors, momenta and other hadronic parameters. To remove the axial vector particle contribution we multiply both the physical and QCD sides of the correlation function by $\frac{p_{1\mu}^* p_{1\nu}^*}{p_1^{*2}}$. The next step is to put the in-medium momenta in terms of the external momenta, vector self-energy and four-velocity vector of the medium like the previous section. We then apply the double Borel transformation with respect to p_1^2 and p_2^2 and use $\mu_1^2 = \mu_2^2 = \mu^2$, $\frac{1}{M^2} = \frac{1}{M_1^2} + \frac{1}{M_2^2}$ and $M_1^2 = M_2^2 = 2M^2$ (the initial and final particles are the same). As a result, we get

$$\hat{\mathbf{B}} \left[\frac{p_{1\mu}^* p_{1\nu}^*}{p_1^{*2}} \Pi_{\mu\nu\lambda}^{Phys} \right] = f_{PS}^{*2} F^{*PS}(Q^2) (2m_{PS}^{*2} + Q^2) e^{-\mu^2/M^2} \left(\frac{p_{1\lambda} + p_{2\lambda} - 2\Sigma_v u_\lambda}{2} \right), \quad (23)$$

which contains three $p_{1\lambda}$, $p_{2\lambda}$ and u_λ structures. We use the structure $p_{1\lambda}$ to extract the electromagnetic form factor of the pseudoscalar K^+ particle. Similarly, we can rewrite the final expression of the QCD side in terms of the same Lorentz structures in Borel scheme as:

$$\begin{aligned} \hat{\mathbf{B}} \left[\frac{p_{1\mu}^* p_{1\nu}^*}{p_1^{*2}} \Pi_{\mu\nu\lambda}^{QCD}(Q^2) \right] &= \Theta_1(M^2, s_0, \rho) p_{1\lambda} \\ &+ \Theta_2(M^2, s_0, \rho) p_{2\lambda} + \Theta_3(M^2, s_0, \rho) u_\lambda, \end{aligned} \quad (24)$$

where $\Theta_{i=1,2,3}(M^2, s_0, \rho)$ are the Borel transformed amplitudes, whose expressions are very lengthy and we prefer to not present their explicit forms here.

By equating the coefficients of the structure $p_{1\lambda}$, from both the physical and QCD sides, the sum rule for the in-medium form factor $F^{*PS}(Q^2)$ is obtained in terms of the in-medium mass and decay constant, the auxiliary parameters M^2 and s_0 as well as other QCD degrees of freedom like the quark masses and quark-gluon in-medium condensates. The vacuum form factor $F^{PS}(Q^2)$ is obtained from $F^{*PS}(Q^2)$ in the limit $\rho \rightarrow 0$.

Let us first discuss the Q^2 dependence of the vacuum form factor $F^{PS}(Q^2)$ in the interval $Q^2 \in [0, 10]$ GeV² and compare the obtained results with the existing experimental data as well as other theoretical predictions. Using all the input parameters we find that the following monopole function explains the form factor $F^{PS}(Q^2)$ (hereafter we omit the super-index PS and add the sub-index K) in terms of Q^2 :

$$F_K(Q^2) = \frac{F_K(0)}{\left[1 + \frac{Q^2}{\alpha} \right]}, \quad (25)$$

where $F_K(0) = 1.044_{-0.031}^{+0.036}$ and $\alpha = 0.801_{-0.113}^{+0.131}$ GeV² are obtained. We plot the vacuum form factor $F_K(Q^2)$ in terms of Q^2 in Fig. (6), where the uncertainties are appeared as a band. We see that the form factors falls with increasing the value of Q^2 and reaches to roughly 10% of $F_K(0)$ value at $Q^2 = 10$ GeV². In Fig. (7), we

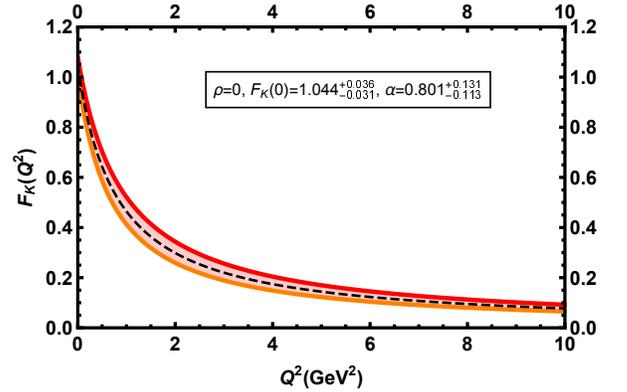


FIG. 6: The vacuum electromagnetic form factor of Kaon in terms of Q^2 considering all the uncertainties of the input parameters.

compare our result on $F_K(Q^2) - Q^2$ with the existing prediction from a model based on the solution of the Bethe-Salpeter equation for the model of NJL with proper-time regularization [31] and Lattice QCD [32] in the interval $Q^2 \in [0, 6]$ GeV². From this figure, we see a nice consistency among our result and the other predictions. In Fig. (8), we compare our result on $|F_K(Q^2)|^2$ with respect to Q^2 at lower values of Q^2 . Within the presented

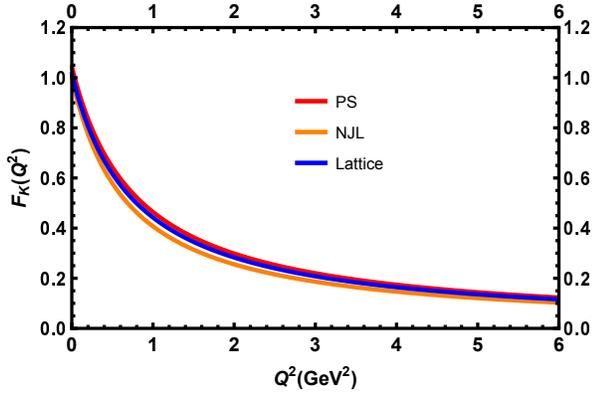


FIG. 7: Comparison of the kaon electromagnetic form factor with different studies (orange solid line [31] and blue solid line [32]).

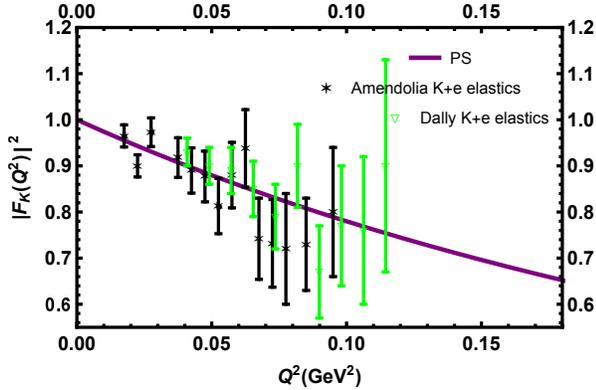


FIG. 8: Variation of $|F_K(Q^2)|^2$ at low Q^2 compared to existing experimental data [22, 23] with $|F_K(Q^2 = 0)|^2$ normalized to one.

uncertainties, we again see a nice agreement between our result and the presented two sets of the experimental data. Finally, in Fig. (9), we compare our result on the behavior of $Q^2 F_K(Q^2)$ with respect to Q^2 in the interval $Q^2 \in [0, 6]$ GeV² with the existing data and predictions of other theoretical and phenomenological models. Although we see a good consistency among all the presented results for $Q^2 \leq 1$ GeV², for $Q^2 > 1$ GeV² we observe overall considerable discrepancies among the theoretical predictions and experimental data that requires more theoretical and experimental studies on the considered quantity at mean values of Q^2 . Our results show relatively a good consistency with the results of Refs. [23, 31, 35] at middle values of Q^2 , as well.

The final subject related to the vacuum analyses is the charge radius. The electromagnetic charge radius of the K meson is obtained from the slope of the electromagnetic form factor at $Q^2 = 0$ value, i.e.,

$$\langle r_K^2 \rangle = -6 \frac{d}{dQ^2} F_K(Q^2) \Big|_{Q^2=0}. \quad (26)$$

Table III compares our result for charge radius in vacuum

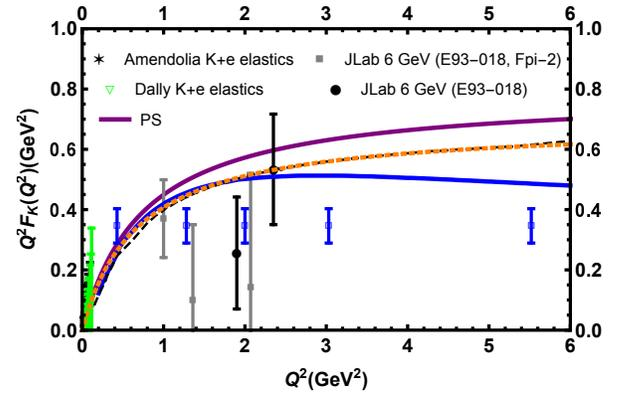


FIG. 9: $Q^2 F_K(Q^2)$ with respect to Q^2 . The result of present study (PS) is represented with the solid purple line. The black stars and green triangles show experimental data taken from Refs. [22, 23]. The filled squares corresponds to kaon electromagnetic form factor from E93-018 and FPI-2. The filled circles data were extracted from the cross section data of Refs. [33, 34]. Blue points with error bars are not data points, they represent the Q^2 range and projected uncertainties of the E12-09-011 JLab experiment [33]. The dashed black curve shows the predictions of Refs. [23, 35]. The dotted orange line is borrowed from Ref. [31]. The solid blue line shows the kaon form factor obtained in Ref. [16].

with the experimental data (world average) and other phenomenological predictions. From this table, we observe that our prediction for r_K is in a nice agreement with the world average experimental data. It is also consistent with the predictions of Refs. [31, 38]. The remaining predictions are slightly higher than our result and the experimental data.

Now, we proceed to discuss the dependence of the electromagnetic form factor and charge radius of the K^+ meson on the density. For this aim, in Fig. (10) we plot the ratio $\frac{F_K^*(Q^2, x)}{F_K(Q^2, 0)}$ as a function of $x = \rho/\rho^{sat}$ at average Q^2 . In Fig. (11), we depict the dependence of $F_K^*(Q^2, x)$ on x at different values of Q^2 and at average values of the auxiliary parameters. From these figures, we observe that the in-medium form factor of kaon starts to increase slightly, however, after $\rho = 1.5\rho^{sat}$ it starts to diminish and sharply goes to zero at a density about $2\rho^{sat}$.

In Fig. (12) we present the variation of the charge radius of the kaon with respect to the density of the medium. From this figure, we observe that, like the in-medium form factor, the radius is slightly increased with increasing in the density, but, it starts to fall after $\rho = 1.5\rho^{sat}$ point and sharply goes to zero at about the density $2\rho^{sat}$. Finally in Fig. (13), we compare our results for the in-medium kaon charge radius, $r_K^*(x)$, with existing predictions of Ref. [39] using NJL model at different densities. The experimental data (red diamond) at zero density is also added for a better comparison. From this figure we see that the behavior of charge radius with respect to the density is similar in our study and Ref. [39] in the interval $x < 1.5$: both predictions growth with in-

Method		r_K
PS	QCDSR	0.54 ± 0.05 fm
[5]	LFCQM	0.636 fm
[17]	DSEs	$\sqrt{0.38}$ fm
[19]	Fit to NA-7 data	$\sqrt{0.39} \leq r_K \leq \sqrt{0.42}$ fm
PDG [26]	Exp	0.560 ± 0.031 fm
[31]	NJL	0.586 fm
[36]	Lattice	$\sqrt{0.380(12)(^{+7}_{-1})(31)}$ fm
[37]	CPT	$\sqrt{0.431 \pm 0.071}$ fm
[38]	RQM	0.57 fm

TABLE III: Experimental result and theoretical predictions of different methods for the kaon vacuum charge radius.

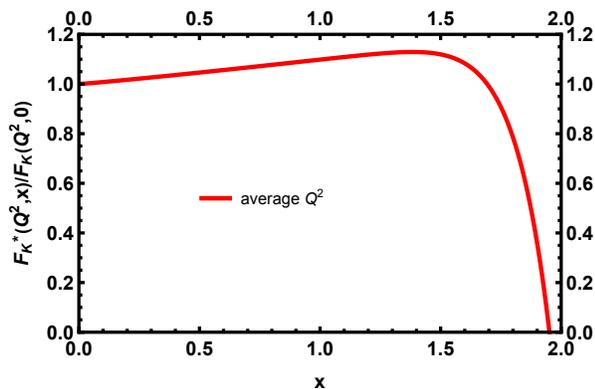


FIG. 10: The variation of the ratio of the density dependent electromagnetic form factor to the vacuum one with respect to the density of the medium at average value of Q^2 .

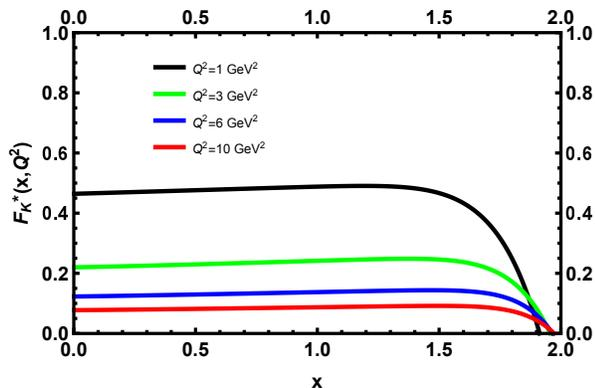


FIG. 11: The variation of $F_K^*(Q^2, x)$ with respect to the density of the medium at different values of Q^2 .

creasing in the density, although our data points growth gradually compared to the data points obtained in [39] which show larger slope. As we previously mentioned, our prediction for the charge radius in vacuum is in a nice agreement with the experimental value in vacuum.

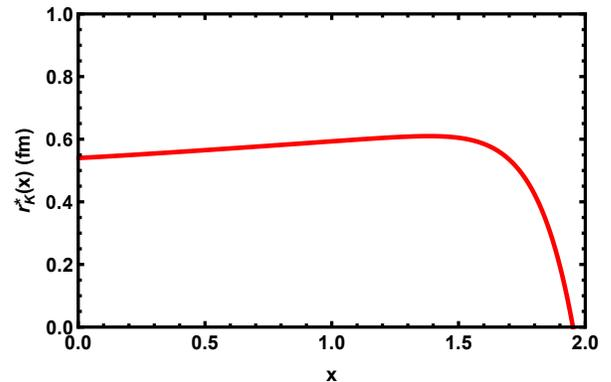


FIG. 12: Variation of the charge radius of the kaon with respect to the density of the medium.

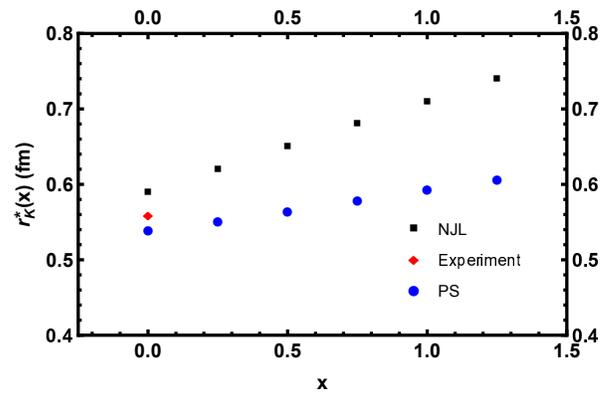


FIG. 13: Comparison of our results for kaon charge radius (blue circle points) with predictions of Ref. [39] using NJL model (black squares) at different densities. We also show the experimental result in vacuum.

IV. SUMMARY AND CONCLUDING NOTES

The spectroscopic parameters as well as the electromagnetic form factor and charge radius of K^+ meson were studied in the context of QCD sum rules both in the vacuum and a medium with finite density. In vacuum, we obtained the mass and decay constant of K^+ meson in a nice consistency with the experimental result and Lattice QCD predictions.

The electromagnetic form factor of this particle was found to have a form of monopole with respect to Q^2 . We investigated the behavior of $F_K(Q^2)$ in terms of Q^2 in a wide range, namely in the interval $Q^2 \in [0, 10]$ GeV^2 . We compared our result with the existing experimental data and other theoretical prediction. We saw a nice consistency among our result and the model based on the solution of the Bethe-Salpeter equation for NJL model with proper-time regularization [31] as well as Lattice QCD [32] in the interval $Q^2 \in [0, 6]$ GeV^2 . Within the presented uncertainties, we also observed a nice agreement among our result and the two sets of the experimental data, namely Amendolia and Dally at low Q^2 s. We also

compared our result on $Q^2 F_K(Q^2)$ with respect to Q^2 in the interval $Q^2 \in [0, 6]$ GeV² with the existing data and predictions of other theoretical and phenomenological models. Although we observed a good consistency among all the presented results for $Q^2 \leq 1$ GeV², for $Q^2 > 1$ GeV² we saw overall considerable discrepancies among the theoretical predictions and experimental data that requires more theoretical and experimental studies. Our results show relatively a good consistency with the results of Refs. [23, 31, 35] at middle values of Q^2 , as well.

We also calculated the charge radius r_K in vacuum and compared the obtained result with the experimental data and other phenomenological predictions. We observed that our prediction for r_K is in a nice agreement with the world average experimental data. It is also consistent with the predictions of Refs. [31, 38].

Regarding the dense medium, we discussed the dependence of the mass and decay constant of K^+ meson on the density of the nuclear medium. To this end, we plotted the dependence of the ratios m_K^*/m_K and f_K^*/f_K on $x = \rho/\rho^{sat}$. We concluded that the mass of K^+ meson increases with the increase in the density, although the rate at lower densities is small. The decay constant linearly decreases with the increase in the density of the medium and it approaches to zero at $\rho \simeq 2.2\rho^{sat}$. At saturation density, the result of the present study for the in-medium mass was compared with the result of Chiral SU(3) model obtained in Ref. [30]: Both show considerable growths with respect to the medium mass value. Our results on the behavior of the in-medium mass and decay constant may help experimental groups aiming to study the in-medium properties of hadrons.

We also discussed the dependence of the electromagnetic form factor and charge radius of the K^+ meson on the density of the nuclear matter. For this aim, we plotted the ratio $\frac{F_K^*(Q^2, x)}{F_K(Q^2, 0)}$ as a function of $x = \rho/\rho^{sat}$ at average Q^2 . We also discussed the dependence of

$F_K^*(Q^2, x)$ on x at different values of Q^2 and at average values of the auxiliary parameters. As a result, we observed that the in-medium form factor of kaon starts to increase slightly, however, after $\rho = 1.5\rho^{sat}$ it starts to diminish and sharply goes to zero at a density about $2\rho^{sat}$.

Finally, we presented the variation of the charge radius r_K^* with respect to the density of the medium. We observed that the radius slightly increases with increasing in the density, however, it starts to fall after $\rho = 1.5\rho^{sat}$ point and approaches to zero at $\rho = 2\rho^{sat}$. We also compared our results for r_K^* at different densities with existing predictions of NJL model [39]. We concluded that the behavior of r_K^* with respect to the density is similar in our study and the NJL model and both predictions growth with increasing in the density. Once more we shall note that our prediction for the charge radius in vacuum is in a nice agreement with the world average experimental data.

The results obtained in the present study, especially, those obtained at finite densities may be checked via different phenomenological models and approaches. They can be useful in analyses of the future related data to be provided by the in-medium experiments. Comparison of the obtained vacuum and in-medium results in the present study with the existing and future experimental data can provide useful information about the nature, internal structure, size and inner charge distribution of the strange meson, K , as well as the nonperturbative nature of QCD as theory of the strong interaction.

ACKNOWLEDGEMENTS

K. Azizi is thankful to Iran Science Elites Federation (Saramadan) for the partial financial support provided under the grant number ISEF/M/400150.

-
- [1] G. R. Farrar and D. R. Jackson, "Pion Form Factor," *Phys. Rev. Lett.* **43**, 246 (1979).
 - [2] V. Bernard and U. G. Meissner, "Electromagnetic Structure of the Pion and the Kaon," *Phys. Rev. Lett.* **61**, 2296 (1988).
 - [3] R. Alkofer, A. Bender and C. D. Roberts, "Pion Loop Contribution to the Electromagnetic Pion Charge Radius," *Int. J. Mod. Phys. A* **10**, 3319-3342 (1995).
 - [4] A. H. Blin, B. Hiller & M. Schaden, "Electromagnetic form factors in the Nambu-Jona-Lasinio model," *Zeitschrift für Physik A Atomic Nuclei* **331**, 75-82 (1988).
 - [5] E. O. da Silva, J. P. B. C. de Melo, B. El-Bennich and V. S. Filho, "Pion and kaon elastic form factors in a refined light-front model," *Phys. Rev. C* **86**, 038202 (2012).
 - [6] B. L. G. Bakker, H. M. Choi and C. R. Ji, "Regularizing the fermion loop divergencies in the light front meson currents," *Phys. Rev. D* **63**, 074014 (2001).
 - [7] D. Melikhov and S. Simula, "Electromagnetic form factors in the light-front formalism and the Feynman triangle diagram: Spin-0 and spin-1 two-fermion systems," *Phys. Rev. D* **65**, 094043 (2002).
 - [8] O. Leitner, J.-F. Mathiot and N. A. Tsirova, "The pion wave function in covariant light-front dynamics," *Eur. Phys. J. A* **47**, 17 (2011).
 - [9] S. J. Brodsky and G. F. de Teramond, "Light-front dynamics and AdS/QCD correspondence: The pion form factor in the space- and time-like regions," *Phys. Rev. D* **77**, 056007 (2008).
 - [10] T. Nguyen, A. Bashir, C. D. Roberts and P. C. Tandy, "Pion and kaon valence-quark parton distribution functions," *Phys. Rev. C* **83**, 062201 (2011).
 - [11] C. A. Dominguez, J. I. Jottar, M. Loewe and B. Willers, "Pion form-factor in the Kroll-Lee-Zumino model,"

- Phys. Rev. D **76**, 095002 (2007).
- [12] A.E. Dorokhov and A.E. Radzhabov and A.S. Zhevlakov, “Pseudoscalar meson transition form factors in nonperturbative QCD approach,” *Nucl.Phys.B Proc.Suppl.* **225-227**, 141-145 (2012).
- [13] J. Bijnens and N. Hermansson Truedsson, “The pion mass and decay constant at three loops in two-flavour chiral perturbation theory,” *JHEP* **11**, 181 (2017).
- [14] J. P. B. C. de Melo, K. Tsushima, B. El-Bennich, E. Rojas and T. Frederico, “Pion structure in the nuclear medium,” *JPhys. Rev. C* **90** (2014) no.3, 035201.
- [15] A. Mishra, A. Kumar, S. Sanyal, V. Dexheimer and S. Schramm, “Kaon properties in (proto)neutron stars,” *Eur.Phys.J.A* **45** 2, 169-177 (2010).
- [16] F. Gao, L. Chang, Y. X. Liu, C. D. Roberts and P. C. Tandy, ‘Exposing strangeness: projections for kaon electromagnetic form factors,” *Phys. Rev. D* **96**, 034024 (2017).
- [17] P. Maris and P. C. Tandy, “The π, K^+ , and K^0 electromagnetic form factors,” *Phys. Rev. C* **62**, 055204 (2000).
- [18] B. Y. Park, J. I. Kim and M. Rho, “Kaons in dense half-Skyrmion matter,” *Phys. Rev. C* **81**, 035203 (2010).
- [19] A. F. Krutov, S. V. Troitsky and V. E. Troitsky, “The K -meson form factor and charge radius: linking low-energy data to future Jefferson Laboratory measurements,” *Eur. Phys. J. C* **77**, 464 (2017).
- [20] N. Solomey, “Measurement of the Charged Kaon Mass,” *Nucl. Phys. B Proc. Suppl.* **210-211**, 185-188 (2011).
- [21] N. Carrasco, P. Dimopoulos, R. Frezzotti, P. Lami, V. Lubicz, F. Nazzaro, E. Picca, L. Riggio, G. C. Rossi and F. Sanfilippo, *et al.* “Leptonic decay constants f_K, f_D , and f_{D_s} with $N_f = 2+1+1$ twisted-mass lattice QCD,” *Phys. Rev. D* **91**, no.5, 054507 (2015).
- [22] E. B. Dally, J. M. Hauptman, J. Kubic, D. H. Stork, A. B. Watson, Z. Guzik, T. S. Nigmanov, V. D. Ryabtsov, E. N. Tsyganov and A. S. Vodopianov, *et al.* “Direct Measurement of the Negative Kaon Form-factor,” *Phys. Rev. Lett.* **45**, 232-235 (1980).
- [23] S. R. Amendolia, G. Batignani, G. A. Beck, E. H. Bellamy, E. Bertolucci, G. Bologna, L. Bosisio, C. Bradaschia, M. Budinich and M. Dell’orso, *et al.* “A Measurement of the Kaon Charge Radius,” *Phys. Lett. B* **178**, 435-440 (1986).
- [24] G. H. S. Yabusaki, J. P. B. C. de Melo, W. de Paula, K. Tsushima and T. Frederico, “In-Medium K^+ Electromagnetic Form Factor with a Symmetric Vertex in a Light Front Approach,” *Few Body Syst.* **59** (2018) no.3, 37.
- [25] K. Azizi and N. Er, “Properties of nucleon in nuclear matter: once more,” *Eur. Phys. J. C* **74**, 2904 (2014).
- [26] P.A. Zyla *et al.* (Particle Data Group), *Prog. Theor. Exp. Phys.* **2020**, 083C01 (2020).
- [27] T. W. Chiu, T. H. Hsieh, J. Y. Lee, P. H. Liu and H. J. Chang, “Pseudoscalar decay constants f_D and f_{D_s} in lattice QCD with exact chiral symmetry,” *Physics Letters B* **624**, 31-38 (2005).
- [28] P. Dimopoulos, R. Frezzotti, M. Garofalo and S. Simula, “ K - and $D_{(s)}$ -meson leptonic decay constants with physical light, strange and charm quarks by ETMC,” *PoS LATTICE2021*, 472 (2021).
- [29] S. Aoki *et al.* [Flavour Lattice Averaging Group], “FLAG Review 2019: Flavour Lattice Averaging Group (FLAG),” *Eur. Phys. J. C* **80**, no.2, 113 (2020).
- [30] A. Mishra, A. K. Singh, N. S. Rawat and P. Aman, “Kaons and antikaons in strong magnetic fields,” *Eur. Phys. J. A* **55** no.7, 107 (2019).
- [31] P. T. P. Hutauruk, I. C. Cloet and A. W. Thomas, “Flavor dependence of the pion and kaon form factors and parton distribution functions,” *Phys. Rev. C* **94**, 035201 (2016).
- [32] C. Alexandrou, S. Bacchio, I. Cloet, M. Constantinou, J. Delmar, K. Hadjiyiannakou, G. Koutsou, C. Lauer and A. Vaquero, “The scalar, vector and tensor form factors for the pion and kaon from lattice QCD,” [arXiv:2111.08135 [hep-lat]].
- [33] T. Horn and C. D. Roberts, “The pion: an enigma within the Standard Model,” *J. Phys. G* **43**, no.7, 073001 (2016).
- [34] M. Coman *et al.* (Jefferson Lab Hall A Collaboration), ‘Cross sections and Rosenbluth separations in $^1\text{H}(e, e'K^+)\Lambda$ up to $Q^2 = 2.35 \text{ GeV}^2$,” *Phys. Rev. C* **81**, 052201(R) (2010).
- [35] M. Carmignotto *et al.* (JLAB FPI-2 and E93-018 Collaboration), “Separated kaon electroproduction cross section and the kaon form factor from 6 GeV JLab data,” *Phys. Rev. C* **97**, 025204 (2018).
- [36] S. Aoki *et al.* [JLQCD], “Light meson electromagnetic form factors from three-flavor lattice QCD with exact chiral symmetry,” *Phys. Rev. D* **93**, 034504 (2016).
- [37] J. Bijnens and P. Talavera, “Pion and kaon electromagnetic form-factors,” *JHEP* **03**, 046 (2002).
- [38] D. Ebert, R. N. Faustov and V. O. Galkin, “Masses and electroweak properties of light mesons in the relativistic quark model,” *Eur. Phys. J. C* **47**, 745-755 (2006).
- [39] P. T. P. Hutauruk and K. Tsushima, “Electroweak properties of kaons in a nuclear medium,” [arXiv:1910.08133 [nucl-th]].